INVESTIGATION OF PHYSICS-BASED APPROACHES FOR WIND TURBINE MODELING AND DESIGN

An Undergraduate Thesis
Presented to
The Academic Faculty

by

Michael Nucci

In Partial Fulfillment
of the Requirements for the Degree
BS Aerospace Engineering Research Option in the
School of Aerospace Engineering

Georgia Institute of Technology
May 2009

INVESTIGATION OF PHYSICS-BASED APPROACHES FOR WIND TURBINE MODELING AND DESIGN

Approved by:

Dr. Lakshmi Sankar, Advisor
School of Aerospace Engineering
Georgia Institute of Technology

Dr. Stephen Ruffin
School of Aerospace Engineering
Georgia Institute of Technology

Date Approved: April 27, 2009

ACKNOWLEDGEMENTS

I would like to thank my mother, father, and brother Steven whose unconditional support has helped me through my educational experience. I would also like to thank my advisor Dr. Lakshmi Sankar, and graduate student Nischint Rajmohan whose guidance greatly helped throughout the lifecycle of my project.

TABLE OF CONTENTS

LIST OF TABLES

LIST OF FIGURES

LIST OF SYMBOLS AND ABBREVIATIONS

c_l	Coefficient of lift
c_p	Coefficient of power
c_t	Coefficient of thrust
P	Power
T	Thrust
V_t	Tip velocity

SUMMARY

Rising oil costs have created a need for a new sustainable energy source. Currently wind energy is beginning to fulfill this need. With many financial incentives being offered for clean energy, wind turbines are a promising green energy source. Wind turbine analysis can be difficult and costly. Accurate spanwise pressure distributions are difficult to measure experimentally, and a full-fledged Navier-Stokes analysis is very computationally expensive.

A comparison of two separate computer codes was performed. These include PROPID, which uses a blade element momentum theory method and empirical data about the wind turbine airfoil. The second method is a Reynolds Averaged Navier-Stokes (RANS) CFD code called windrotor2 which also was used to predict the performance of the NREL Phase VI rotor. Once the codes were validated they were then used to predict the performance of new rotor designs.

This research shows that PROPID can be used as a surrogate model for turbine analysis and design. PROPID can be shown to predict performance that is on par with CFD methods in terms of accuracy, but takes only a fraction of the time to perform the analysis. PROPID can also be shown to accurately predict the performance of new turbine configurations as long as empirical data is readily available.

CHAPTER 1

INTRODUCTION

With continually rising oil costs and an uncertain quantity of oil, it is time to find a new sustainable energy source. In fact, the United States has a goal of reducing its oil consumption by twenty percent over the next ten years [1], and many states are offering financial incentives for using green energy [2]. Wind energy is a promising idea because it is environmentally friendly and is available in many areas. Currently it is the main contributor of new zero-emissions energy to the United States energy supply [3]. Although the initial capital required to build a wind farm is large, the cost of the energy goes down each year that the farm is in service [4]. A typical wind turbine can be in service for about twenty years. At the heart of the wind turbine is the rotor, which is used to extract energy from the wind. As the efficiency of the rotor increases, the amount of energy that the turbine is capable of extracting from the wind increases, and in turn the cost of energy decreases. Therefore it is extremely beneficial to design the most efficient rotor possible.

Analysis of wind turbine blades can be a costly process. It is not easy to experimentally measure a detailed spanwise distribution of aerodynamic characteristics of interest such as c_p, c_l, c_t, etc. Nor is it easy to measure any data on a full size turbine blade because very few wind tunnels worldwide are capable of housing such large objects. Analyzing turbine performance computationally is in many ways more practical; however it can be costly as well. Complex boundary layer and turbulent flow interactions require the use of sophisticated computational fluid dynamic (CFD) codes

with turbulent flow models to obtain exact results. These codes can take days to completely converge upon a solution, and they tie up resources in the mean time.

The National Renewable Energy Lab has conducted numerous experiments on wind turbine performance. One particular experiment, the Phase VI rotor [5], is of particular interest to the wind turbine community. This rotor was tested at the NASA Ames Research Center in Moffitt Field, California. The rotor was tested inside of the 80' x 120' wind tunnel located on the premises. The wind tunnel was capable of producing a flow up to 115 miles per hour. Several aerodynamic measurements were taken including the power generated by this rotor, which is the primary focus of this research.

As an alternative to computationally expensive CFD codes, Dr. Michael Selig developed PROPID [6], which uses blade element momentum theory (BEMT) and empirical airfoil data, to compute a solution in a much quicker time. In this project, PROPID, along with a CFD code developed by Tongchitpakdee [7], will be verified against the experimental results obtained during the NREL tests for the Phase VI rotor.

Once the verification is complete, PROPID will be used as a wind turbine blade design tool to analyze a series of changes to the twist distribution of the Phase VI rotor. Any performance increase suggested by these changes will then be verified using the CFD code. If the CFD code and PROPID predict the same results, then it will be clear that PROPID is a valid surrogate model for wind turbine design.

The importance of this work is that it will allow for the savings of countless hours of computer time without the sacrifice of accuracy. PROPID is capable of analyzing the performance of a wind turbine in a few seconds as long as empirical data is available. The CFD code takes much longer; the exact time depends on the grid size, but at least

thirty hours are needed to converge on an accurate result. If PROPID proves to be a valid surrogate model, then it can be used as a design tool to analyze new turbine configurations for which the airfoil data is known.

CHAPTER 2

LITERATURE REVIEW

This work is an extension of the myriad projects dealing with the NREL Phase VI rotor and turbine performance prediction. Many researchers have examined the feasibility of computational prediction of performance for the Phase VI rotor using an assortment of methods.

Sorensen [8] shows that an incompressible Reynolds-averaged Navier-Stokes solver can provide good quality results for 3D aerodynamic effects of a turbine blade at 0° yaw angle. The code predicted results within one standard deviation of the experimental results for all wind speeds of interest. This method does have some difficulty predicting performance during unstable flow, which leads to flow separation on the turbine blade.

Gupta [9] used a free-vortex wake method (FVM) to predict performance. This method predicted the thrust and power output of the blade very well. The spanwise variation of loads also showed good agreement to the experimental values. The free-vortex wake method did have trouble predicting the onset of dynamic stall which lead to the under prediction of the azimuthal variation of some loads.

Many CFD codes have been proven to accurately predict wind turbine performance without need for empirical data about the turbine blade. However, this accuracy comes with a steep penalty in computational cost. It is therefore in the best interest of the wind turbine community to find a computationally cheaper method to obtain accurate results.

Park [10] used the commercially available CFD code FLUENT with various turbulence models to analyze the Phase VI rotor. In the interest of saving computational time, models of smaller scales were also tested. It was found that the CFD code could be

used on a smaller scale model to save time, and still provide accurate results of wind turbine performance. This is similar to what is done in the experimental community when a smaller model is tested in a wind tunnel and results are matched with the help of Reynolds number.

Schmitz [11] devised a computational scheme that would use a computationally intensive CFD method in the near-field of the turbine blade, but would use a much cheaper vortex panel solver in the far-field. This method uses the Navier-Stokes equations to capture the 3D characteristics of the flow and the non-dissipative vortex panel method to analyze the trailing vortex wake. This method provided very good agreement with experimental results for attached flow, and was computationally much cheaper than a full Navier-Stokes solution. However, the method had trouble predicting performance for separated flow.

Massouh [12] developed a hybrid model similar to that of Schmitz [10] to predict performance. This method combined the computationally intensive Reynolds averaged Navier-Stokes (RANS) method with the blade element method (BEM) to represent the turbine blade with less nodes. This method significantly reduced the computational complexity of the problem to such a degree that now a wind farm may be analyzed so that the wake interactions between turbines can be researched.

Duque [13] uses a computationally cheap vortex-lattice code to analyze the performance of the turbines, and compares this to an expensive RANS code. The vortex-lattice code requires 2D airfoil data and is similar to PROPID in this sense. This work shows that the vortex-lattice code does a good job predicting the non-stalled performance of the blade, but fails to accurately predict the stalled performance even with stall models. The RANS code is able to accurately predict both the stalled and non-stalled performance of the turbine.

The current work also uses a RANS code, this one developed by Tongchitpakdee [7]. This code was developed specifically for wind turbines and is called windrotor2.

The Navier-Stokes equations are solved with a stable dissipative time-marching scheme which allows the code to achieve second order accuracy in time. The method used is called the Lower-Upper Symmetric Gauss-Seidel implicit scheme. This method is widely used in solving the Navier-Stokes equations. To model turbulent flow the code uses the Spalart-Allmaras turbulence model.

The current work goes along with the goals of Massouh [12] and Duque [13]. A RANS method will be used to solve the governing equations [7,14]. Using a blade element momentum theory (BEMT) method called PROPID [15] and empirical data on the S809 airfoil, performance predictions will be made. These two methods will be compared to experimental results for the NREL Phase VI rotor and it will be determined if the computationally cheaper PROPID may be used as a surrogate model for the RANS method. Then PROPID will be validated as a design tool by determining if the CFD code and PROPID prediction agree on the performance of a newly designed turbine blade.

CHAPTER 3

METHODOLOGY

In the current work the PROPID [6] code was used to predict the power production of the NREL Phase VI rotor. The Phase VI rotor was developed specifically for experimental tests, and is widely believed to provide accurate experimental data. The baseline Phase VI rotor has two blades with a radius of 5.03 meters, rotates at 72 RPM, uses the S809 airfoil throughout its span, and operates at a 0° yaw angle. PROPID requires empirical data for the S809 airfoil to do the analysis, and this data is provided in Appendix A. The Phase VI rotor also uses a tapered blade. The chord-length distribution can be seen in Appendix B.

PROPID predicts the power production of this turbine at numerous wind speeds. These results were compared to the experimentally obtained data for the rotor [5] to validate the accuracy of PROPID.

The twist distribution of the S809 airfoil used on the Phase VI rotor was changed in an attempt to provide more power. Both a linear and parabolic twist distribution were used with a tip twist of near -7°. PROPID can model these changes with a simple edit to the input file. Table 3.1 shows the twist distribution for the various cases.

Table 3.1. Twist distribution for baseline, linear, and parabolic cases.

Radial Distance (m)	Baseline Twist (deg)	Linear Twist (deg)	Parabolic Twist (deg)
0.000	0.00	0.00	0.00
0.724	0.00	0.00	0.00
0.838	30.00	16.34	8.02
0.968	27.59	15.61	7.88
1.258	20.05	14.00	7.50
1.522	14.04	12.53	7.06
1.798	9.67	10.99	6.52
2.075	6.75	9.45	5.88
2.352	4.84	7.91	5.16
2.628	3.48	6.37	4.34
2.905	2.40	4.83	3.43
3.181	1.51	3.29	2.44
3.458	0.76	1.75	1.35
3.735	0.09	0.21	0.17
3.772	0.00	0.00	0.00
4.011	-0.55	-1.33	-1.10
4.288	-1.11	-2.87	-2.46
4.565	-1.55	-4.41	-3.92
4.841	-1.84	-5.95	-5.46
5.030	-2.00	-7.00	-6.56

These results needed to be compared to the predicted results of the RANS CFD code. The RANS code requires a computational grid to be generated around the turbine. The generated grid [7,14] had dimensions of 129 points in the blade wrap-around direction, 88 points in the spanwise direction of the blade, and 41 points in the normal direction. It was for a single blade of the NREL Phase VI turbine.

The RANS code was used several times to solve for the turbine performance at various wind speeds of interest. The wind speed was specified by changing the value for the advance ratio in the input file. The thrust and power predicted by the code were compared to the experimental results to verify the accuracy of the solver. The CFD code outputs coefficients of thrust and torque. Equations 1 and 2 were used to convert these coefficients into their respective dimensional values.

$$C_T = \frac{T}{\pi R^2 \rho V_t^2} \tag{1}$$

$$C_Q = \frac{P}{2\pi R^2 \rho V_t^3} \tag{2}$$

The scale factor "2" appears in the denominator of Equation 2 because this factor provided better agreement with the experimental data. It is believed that the need for this "2" arises from the way in which parameters were non-dimensionalized within the CFD source code. Further analysis can be done to verify this. Once the thrust and power are calculated using Equations 1 and 2, they must be multiplied by two because there are two blades in the baseline Phase VI rotor, and the grid is only modeling one blade.

Subsequently the blade with a linear twist distribution, which was previously analyzed with PROPID, was tested with the RANS code. This was done by generating a new grid with the new twist distribution. This new grid was then solved with the RANS solver. Again, Equations 1 and 2 were used to determine the dimensional results, and the new blade's power output was compared to the original NREL Phase VI rotor.

CHAPTER 4

RESULTS AND DISCUSSION

PROPID was used to predict the performance of the NREL Phase VI rotor baseline case. The input file for this case can be seen in Appendix C, and the experimental power data can be seen in Appendix D. PROPID does a great job of predicting the power output at low wind speeds (non-stalled conditions (Figure 4.1).

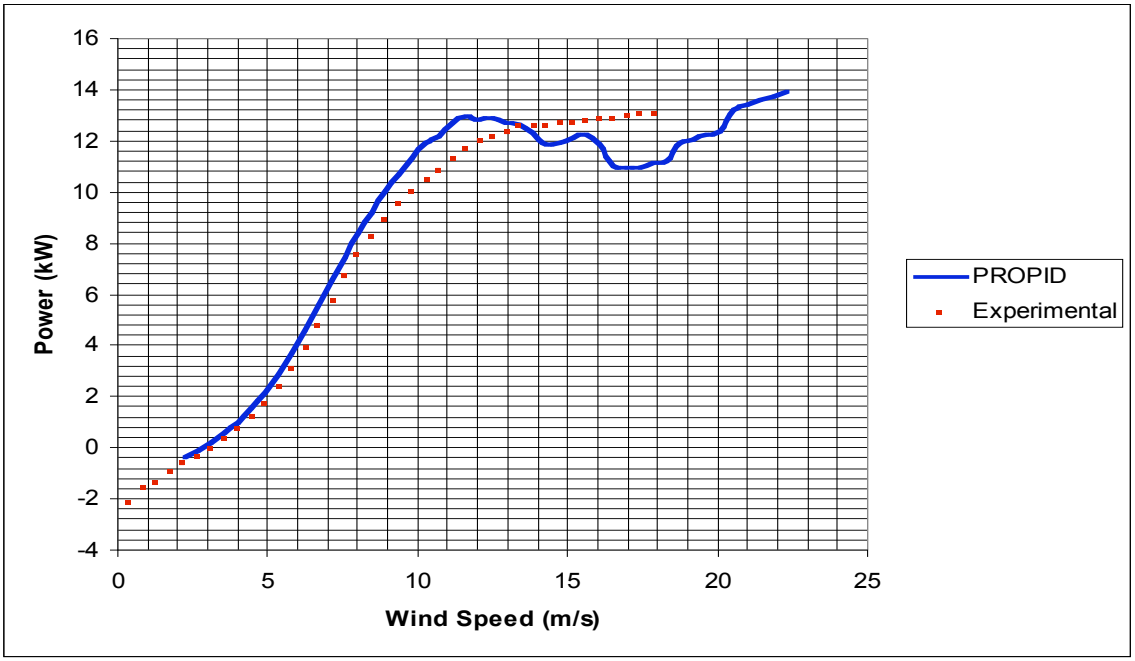

Figure 4.1: Verification of PROPID for power.

At low speeds the prediction very nearly matches the experimental values, but consistently overpredicts performance. It is clear that PROPID is not valid for speeds over 12 m/s because it cannot account for the effects of separated flow. This is why the power predicted by PROPID at higher speeds is not a smooth curve like the experimental values.

For predicting thrust, PROPID does not do as well as it does for power (Figure 4.2). The experimental thrust data can be found in Appendix G.

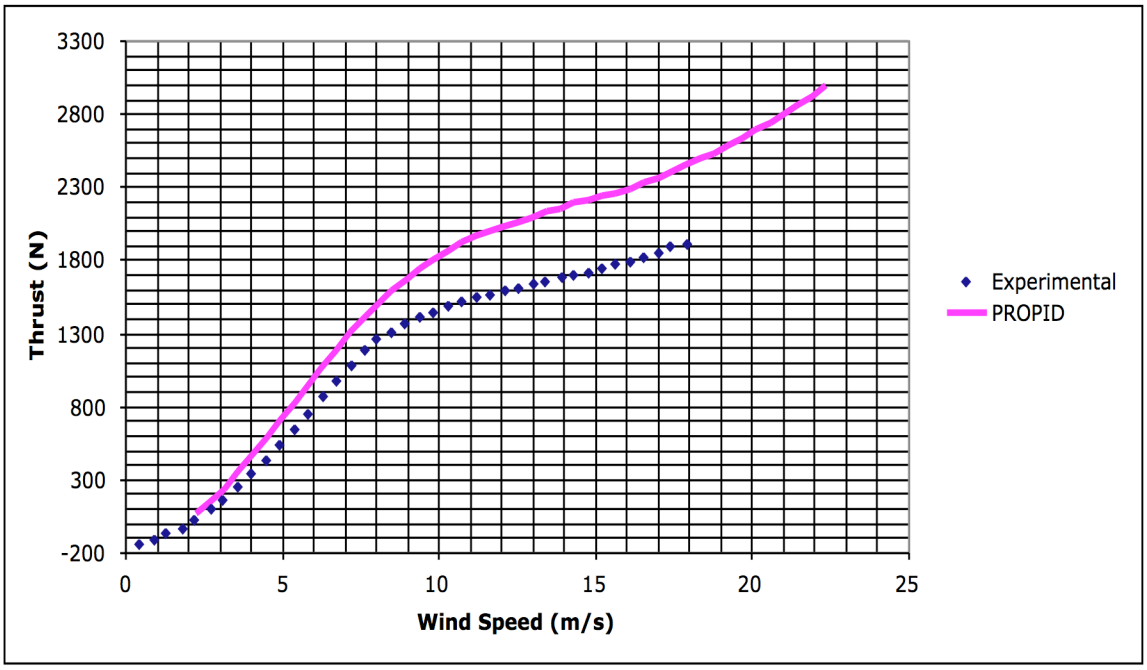

Figure 4.2: Verification of PROPID for thrust.

PROPID shows the same qualitative trend as the experimental data, but consistently over predicts the thrust value. As the wind speed increases PROPID does an increasingly worse job of predicting the thrust.

A linear twist distribution with -7 degree twist at the tip and a parabolic twist distribution with a -6.56 degree twist at the tip were analyzed with PROPID. The twist distributions of the linear and parabolic cases are shown in Table 3.1. To analyze these cases, the PROPID input file shown in Appendix C was modified with the only change being that the twist distribution was changed. In the region where PROPID is valid (non-stall), the three blades perform basically the same (Figure 4.3). However, as the blades approach the stall speed (~11 m/s) the linear blade shows a slight advantage.

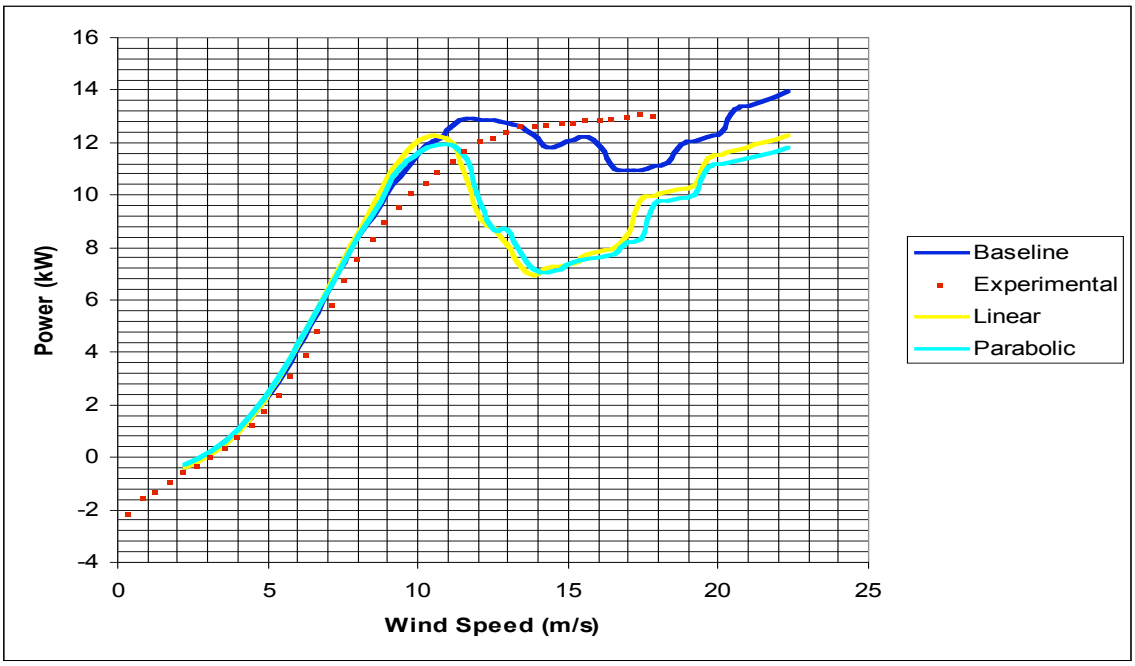

Figure 4.3: PROPID proposed design changes.

The large decrease in performance of the linear and parabolic blades after 11 m/s cannot be trusted because PROPID cannot model flow separation. Therefore PROPID is suggesting that the linear blade will perform at least the same, and possibly better than the baseline blade for wind speeds below stall. The stall performance of the blade can only be determined with the RANS code.

The CFD code could now be verified against NREL experimental data. Before the code can be solved, a computational grid must be generated around the blade. An O-grid with one zone was developed [7, 14]. The input file for the grid generator can be seen in Appendix E. Once the grid is generated, the solver may be used to compute the solution. A sample input for the solver can be found in Appendix F. The advance ratio term in the input file is used to vary the freestream speed.

The RANS solver was then verified by comparing its thrust prediction with the experimentally measured values. The experimentally measured thrust values can be seen

in Appendix G. The predicted thrust very closely matched the experimental values (Figure 4.4).

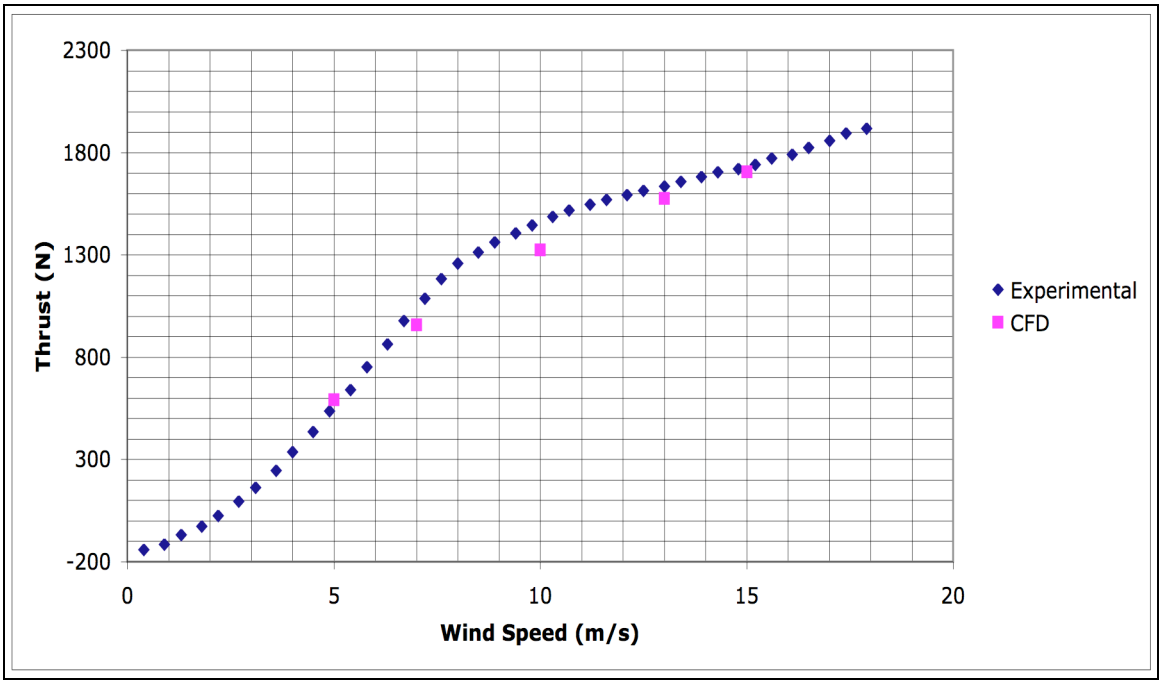

Figure 4.4: Comparison of experimental and CFD predicted thrust.

Figure 4.4 shows that the CFD code does an extremely good job of predicting the thrust at most wind speeds. It has a little difficulty around 10 m/s due to flow separation, but overall the agreement between predicted and measured values is quite good.

The CFD code power prediction is also compared with the experimental results (Figure 4.5).

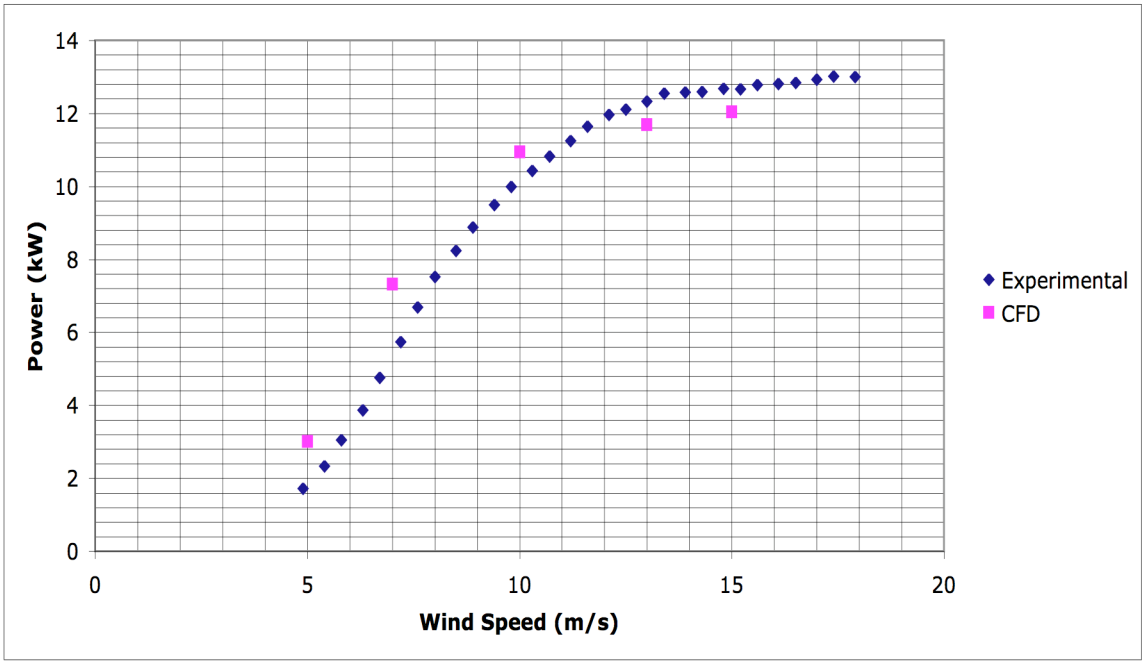

Figure 4.5: Comparison of CFD predicted power to experimental results.

Figure 4.5 shows that the CFD code is capable of predicting the behavior of the wind turbine even without the aid of empirical data. Similar to PROPID, it does tend to over predict the wind turbine performance in the regions of lower velocity. Using a linear interpolation between data points the percent error for the PROPID and the CFD method could be determined (Table 4.1).

Table 4.1: Error of PROPID and CFD methods at wind speeds of interest.

Wind Speed (m/s)	Exp Power (kW)	PROPID Power (kW)	CFD Power (kW)	PROPID % Error	CFD % Error
5	1.84	2.29	3.00	24%	63%
7	5.35	6.22	7.32	16%	37%
10	10.18	11.55	10.94	14%	7%
13	12.34	12.72	11.69	3%	-5%
15	12.68	12.05	12.04	-5%	-5%

Clearly both methods over predict performance in the low wind speed region. The CFD method does a slightly better job predicting the onset of flow separation as evidenced by

a lower error near the 10 m/s wind speed. Table 4.1 shows that both methods are valid for predicting the general behavior of a wind turbine. The CFD method has the capability to provide even more accurate results. Further work on grid sensitivity studies and turbulence models will likely lead to more accurate results for power prediction.

Now that both PROPID and the CFD method have been verified, the CFD method can be used to predict the performance of the linear twist model that PROPID suggested would be an improvement. To do this a new grid must first be generated. This was done by modifying the grid generator input file found in Appendix E by changing the twist distribution to that found for the linear model in Table 3.1.

Once the new grid had been generated, the CFD code could be run (Figure 4.6).

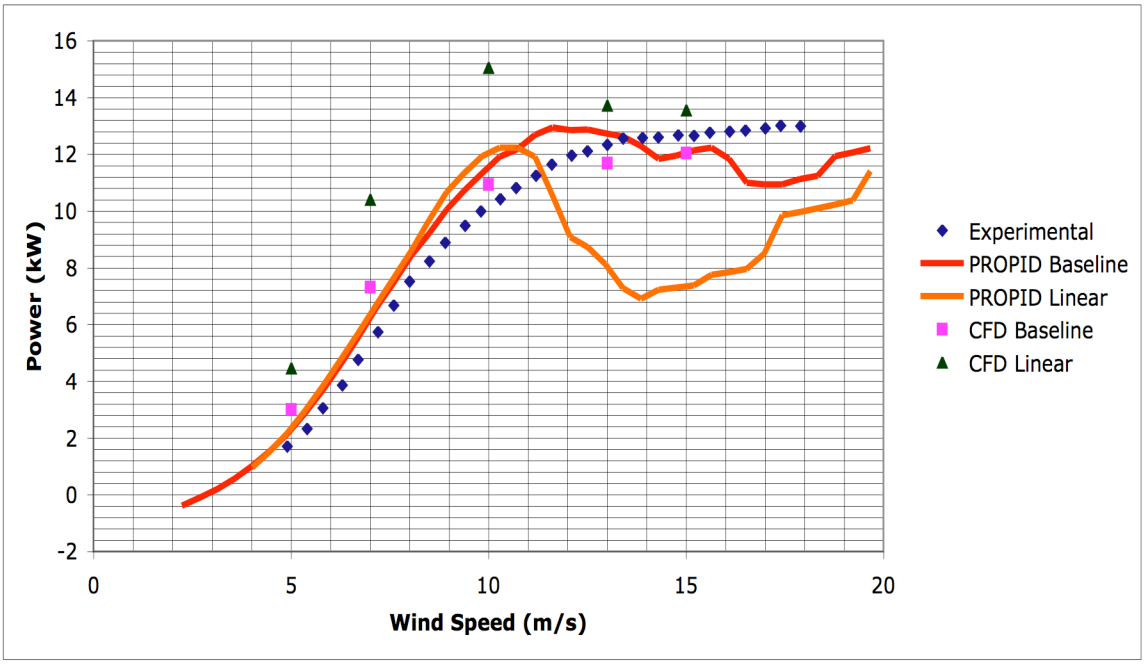

Figure 4.6: Prediction of linear twist model compared to baseline.

Clearly the RANS CFD code qualitatively validates the claims of PROPID. The CFD code also predicts an improvement in performance for the linear twist model compared to the baseline model; however it shows a far greater improvement with twist.

It also predicts that the blade's stall performance will not be as bad as anticipated by PROPID.

CHAPTER 5

CONCLUSIONS AND RECOMMENDATIONS

In this research the BEM theory wind turbine code PROPID was validated for the power prediction of the NREL Phase VI rotor, and then used as a design tool to improve performance. A RANS CFD solver was validated for the same NREL data and used to assess the validity of the design improvement suggested by PROPID.

The results shown here prove that PROPID is a valid surrogate model for design and analysis of wind turbines. PROPID was used to predict the power production of new wind turbine blades with linear and parabolic twist distributions. A RANS CFD code was used to confirm PROPID's prediction for the improved performance of a new blade with a linear twist distribution over the baseline model. Both PROPID and the CFD code showed the same trend in performance improvement, but the CFD code predicted a greater performance change due to the twist.

However, it was also shown that PROPID cannot predict the effects of flow separation well, and results in this flow regime are poor. The RANS code can predict the separated flow much better.

The use of PROPID for wind turbine analysis can provide results that are on par with CFD methods in terms of accuracy, but at a very small fraction of the computational cost. For any wind turbine analysis for which the necessary empirical data is readily available, PROPID should strongly be considered for an analysis tool.

In future work it is recommended that grid sensitivity studies be performed and multiple turbulence models be tested for the CFD code. This analysis will likely lead to the code producing more accurate results for power prediction.

APPENDIX A

S809 AIRFOIL EMPIRICAL DATA

S809 (Eppler data with modifications near stall)
SMOOTH
1
750000 #Reynold Number
21 #Data Sets

Alpha	Cl	Cd
-8.20	-.560	0.0233
-6.10	-.640	0.0131
-4.1	-0.429	0.0134
-2.1	-0.202	0.0119
0.1	0.059	0.0122
2	0.294	0.0116
4.1	0.539	0.0144
6.2	0.789	0.0146
8.1	0.970	0.0162
10.2	1.134	0.0274
11.3	1.210	0.0303
12.1	1.279	0.0369
13.2	1.375	0.0509
14.2	1.455	0.0648
15.3	1.539	0.0776
16.3	1.604	0.0917
17.1	1.639	0.0994
18.1	1.676	0.2306
19.1	1.691	0.3142
20.1	1.748	0.3186
30	2.484	0.4784

APPENDIX B

NREL Phase VI Rotor Chord-Length Distribution [5]

Radial Distance (m)	Chord (m)	Twist (degrees)
0	Hub Diameter	0
0.724	Hub Diameter	0
0.838	0.727	30
0.968	0.730	27.59
1.258	0.737	20.05
1.522	0.710	14.04
1.798	0.682	9.67
2.075	0.654	6.75
2.352	0.626	4.84
2.628	0.598	3.48
2.905	0.570	2.4
3.181	0.542	1.51
3.458	0.514	0.76
3.735	0.486	0.09
2.772	0.483	0
4.011	0.459	-0.55
4.288	0.431	-1.11
4.565	0.403	-1.55
4.841	0.375	-1.84
5.030	0.356	-2

APPENDIX C

PROPID Verification Input File

```
# verify.in
# Modeled loosely after the AOC 15/50, analysis case
# Stall Regulated Turbine

# Basic input
MODE 1.0          # wind turbine
INCV 0.0          # wind turbine mode (use TSR in analysis)
LTIP 1.0          # use tip loss model
LHUB 1.0          # use hub loss model
IBR 1.0           # use brake state model
ISTL 1.0          # use viterna stall model
USEAP  1.0        # use swirl suppression
WEXP 0.0000       # boundary layer wind exponent
NS_NSEC 10.0  1.0   # number of blade elements/number of sectors
IS1   1.0         # first segment used in analysis
IS2  10.0         # last segment used in analysis
BE_DATA 1         # printout blade element data
SH 0.0            # no shaft tilt effects on crossflow
RHO 0.0023769     # air density (slugs/ft^3)

# Geometry
HUB 0.07          # normalized hub cutout ****(changed) 14.25/198
HH 3.372          # normalized hub height ****(changed) 6000/16.5
BN 2              # blade number ****(changed)
CONE 3.4          # cone angle of rotor (deg) ****(changed)
RD 16.5           # radius (ft)
CH_TW   # Normalized chord and twist distribution ****(changed)
0.144   0.00
0.141   30.00
0.136   9.67
0.124   4.84
0.113   2.40
0.102   0.76
0.096   0.00
0.086   -1.11
0.075   -1.84
0.071   -2.00

# No stall models used
# CORRIGAN_EXPN 1

# Corrigan inputs are not used since stall model is off
```

```
AIRFOIL_MODE    4
1
s809.pd
.24  13.  2.484  0  30

# airfoil family 1 with 4 airfoils
# r/R-location and airfoil index
AIRFOIL_FAMILY   2
   0.0000   1
   1.0000   1

# use the first airfoil family (the one above)
USE_AIRFOIL_FAMILY   1

# Enforce tip loss model to always be on
TIPON
# Use the Prandtl tip loss model,
# not the original modified model.
TIPMODE 2

# Design point: 72 rpm, 5 deg pitch, 16 mph ***(changed)
DP   1  72   5.00   16.000  2

# Initiate design (does some preliminary work before analysis)
IDES

# Determine the rotor power, cp, and thrust curves (2D_SWEEP)
#
# use pitch setting from design point (DP) 1
PITCH_DP 1
# use rpm from design point (DP) 1
RPM_DP 1
# sweep the wind from 5 to 50 mph in increments of 1 mph
WIND_SWEEP 5  50   1  2
# perform the sweep
2D_SWEEP
# write out
# 40 - power curve (kW) vs wind speed (mph)
# 45 - cp vs TSR
# 51 - rotor thrust curve
WRITE_FILES  40 45 51

# Compute the gross annual energy production
# Output the data to file: gaep.dat
#
# Initial avg wind speed - 14 mph
```

```
# Final   avg wind speed - 18 mph
# Step                -  2 mph
# Cutout              - 45 mph
#
# 100% efficiency
GAEP  14 18 2 45
#
# 15 mph only, 85% efficiency
# GAEP  15 15 1 45 .85

# Obtain aero distributions along the blade (1D_SWEEP)
#
PITCH_DP 1
RPM_DP 1
WIND_SWEEP 5 30 5 1
1D_SWEEP
# write out
# 75 - blade l/d  dist
# 76 - blade Re   dist
# 80 - blade alfa dist
# 85 - blade cl   dist
# 90 - blade a    dist
#WRITE_FILES 75 76 80 85 90

# Write out
# 95 - chord dist (ft-ft)
# 99 - alfa  dist (ft-deg)
#WRITE_FILES 95 99

# Write out the rotor design parameters to file ftn021.dat
DUMP_PROPID

*
```

APPENDIX D

NREL Phase VI Rotor Power Data [5]

Wind Speed (m/s)	Power (kW)
4.9	1.72
5.4	2.34
5.8	3.06
6.3	3.87
6.7	4.77
7.2	5.74
7.6	6.69
8	7.53
8.5	8.24
8.9	8.89
9.4	9.5
9.8	10
10.3	10.44
10.7	10.83
11.2	11.25
11.6	11.65
12.1	11.97
12.5	12.11
13	12.34
13.4	12.56
13.9	12.58
14.3	12.6
14.8	12.68
15.2	12.67
15.6	12.78
16.1	12.81
16.5	12.85
17	12.93
17.4	13.02
17.9	13

APPENDIX E

CFD Verification Grid Generator Input File

```
 This actually IS the CARDONNA TUNG. AR=7. JUNE 93
 IRSTRT   IWRITE  IPLTFILE   IWAKE  IGWRITE   IPRTCP   IPLOT3D
    0        0        1        0        0     3000        1
  IM0      JM0      KM0      JTIP       DT       WW     ALFA
  181      100       65       70    0.001     0.01      0.0
 ITEL     ITEU    ISTDY    ITURB    LTHIN    LOCDT
  41      141        1        1        0        1
  DN1      DN2      YB       DY1    dtmax    dtmin    WWIF
.0005    .0005     1.0     0.004      0.1    0.003      5.
  NSTP    AMTIP   REYTIP      DX1       XB       dummy
  1000     0.44     1.5     0.003     6.0        0
  ADVRAT   PSI0    IFIXW     IGW0   IGREAD   RESIORD    BVI
  0.0000   90.0       0        1        0        4.       FALSE
  XTRN     ROE
  0.       0
  INITKE   IPRO    IKEPS    IFACT1   DTFACT1
  0        1000     0        1000     0.001
J30   J47   J63   J80   J95
18    30    39    49    60
y(j), j ===> 1 .. Jtip
        0.02
        0.04
        0.06
        0.08
        0.09
        0.095
        0.0975
        0.1
        0.102465623
        0.105191191
        0.108966124
        0.113803245
        0.119703155
        0.126657763
        0.134652409
        0.143667251
        0.153678232
        0.164657798
        0.17657543
        0.189398071
        0.203090462
        0.217615423
```

0.232934081
0.24900607
0.265789699
0.283242099
0.301319353
0.31997661
0.339168194
0.358847691
0.378968042
0.399481621
0.420340309
0.441495564
0.46289849
0.484499897
0.506250365
0.528100301
0.55
0.571899699
0.593749635
0.615500103
0.63710151
0.658504436
0.679659691
0.700518379
0.721031958
0.741152309
0.760831806
0.78002339
0.798680647
0.816757901
0.834210301
0.85099393
0.867065919
0.882384577
0.896909538
0.910601929
0.92342457
0.935342202
0.946321768
0.956332749
0.965347591
0.973342237
0.980296845
0.986196755
0.991033876
0.994808809

0.997534377
1
TOTAL NUMBER OF INPUT STATIONS, COLLECTIVE PITCH (DEG),IN. TWI.
18 5.00
ZS(K) XL YL CHORD THICK TWIST NEWSEC
1.7350 -0.3473 0.0 0.6946 1.0 30.0 1
YSYM FNU FNL
0 61 62
XPOINT ZPOINT
0.000000 0.000000
0.001400 0.004980
0.005365 0.008850
0.009330 0.012720
0.016270 0.017170
0.023210 0.021620
0.032720 0.026530
0.042230 0.031440
0.054010 0.036720
0.065790 0.041990
0.079520 0.047500
0.093250 0.053010
0.108610 0.058550
0.123970 0.064080
0.140745 0.069380
0.157520 0.074670
0.175570 0.079570
0.193620 0.084470
0.212685 0.088870
0.231750 0.093260
0.251520 0.096930
0.271290 0.100600
0.291585 0.103250
0.311880 0.105890
0.332580 0.107280
0.353280 0.108660
0.374345 0.108540
0.395410 0.108420
0.416865 0.106630
0.438320 0.104840
0.460330 0.101200
0.482340 0.097560
0.505355 0.092270
0.528370 0.086970
0.552500 0.080700
0.576630 0.074420
0.601560 0.067770

0.626490 0.061120
0.651795 0.054520
0.677100 0.047920
0.702310 0.041750
0.727520 0.035580
0.752100 0.030120
0.776680 0.024660
0.800080 0.020130
0.823480 0.015590
0.845125 0.012090
0.866770 0.008590
0.886110 0.006150
0.905450 0.003700
0.921985 0.002230
0.938520 0.000750
0.951805 0.000110
0.965090 -0.000540
0.974775 -0.000595
0.984460 -0.000650
0.990290 -0.000445
0.996120 -0.000240
0.998060 -0.000120
0.999030 -0.000060
1.000000 -0.000000
XPOINT ZPOINT0
0.000000 0.000000
0.000370 -0.002750
0.003060 -0.007205
0.005750 -0.011660
0.011005 -0.016495
0.016260 -0.021330
0.023920 -0.026345
0.031580 -0.031360
0.041525 -0.036395
0.051470 -0.041430
0.063575 -0.046375
0.075680 -0.051320
0.089790 -0.056070
0.103900 -0.060820
0.119850 -0.065270
0.135800 -0.069720
0.153415 -0.073790
0.171030 -0.077860
0.190115 -0.081455
0.209200 -0.085050
0.229535 -0.088090

0.249870 -0.091130
0.271230 -0.093535
0.292590 -0.095940
0.314740 -0.097635
0.336890 -0.099330
0.359560 -0.100210
0.382230 -0.101090
0.405160 -0.101050
0.428090 -0.101010
0.450965 -0.099720
0.473840 -0.098430
0.496945 -0.095400
0.520050 -0.092370
0.544030 -0.087965
0.568010 -0.083560
0.592740 -0.078675
0.617470 -0.073790
0.642325 -0.068910
0.667180 -0.064030
0.691620 -0.059325
0.716060 -0.054620
0.739600 -0.050200
0.763140 -0.045780
0.785350 -0.041695
0.807560 -0.037610
0.828050 -0.033890
0.848540 -0.030170
0.866955 -0.026760
0.885370 -0.023350
0.901500 -0.020145
0.917630 -0.016940
0.931430 -0.013975
0.945230 -0.011010
0.956610 -0.008505
0.967990 -0.006000
0.976635 -0.004225
0.985280 -0.002450
0.990755 -0.001495
0.996230 -0.000540
0.998115 -0.000270
1.000000 0.000000

ZS(K)	XL	YL	CHORD	THICK	TWIST	NEWSEC
2.0041	-0.4761	0.0	0.9522	1.0000	27.59	0

ZS(K)	XL	YL	CHORD	THICK	TWIST	NEWSEC
2.6046	-0.76259	0.0	1.5259	1.0000	20.05	0

ZS(K)	XL	YL	CHORD	THICK	TWIST	NEWSEC

3.1511 -0.735 0.0 1.4700 1.0000 14.04 0
ZS(K) XL YL CHORD THICK TWIST NEWSEC
3.7226 -0.706 0.0 1.4120 1.0000 9.67 0
ZS(K) XL YL CHORD THICK TWIST NEWSEC
4.2961 -0.677 0.0 1.3540 1.0000 6.75 0
ZS(K) XL YL CHORD THICK TWIST NEWSEC
4.8696 -0.64805 0.0 1.2961 1.0000 4.84 0
ZS(K) XL YL CHORD THICK TWIST NEWSEC
5.4410 -0.619 0.0 1.2381 1.0000 3.48 0
ZS(K) XL YL CHORD THICK TWIST NEWSEC
6.0145 -0.59005 0.0 1.1801 1.0000 2.40 0
ZS(K) XL YL CHORD THICK TWIST NEWSEC
6.5859 -0.5611 0.0 1.1222 1.0000 1.51 0
ZS(K) XL YL CHORD THICK TWIST NEWSEC
7.1594 -0.5321 0.0 1.0642 1.0000 0.76 0
ZS(K) XL YL CHORD THICK TWIST NEWSEC
7.7329 -0.5031 0.0 1.0062 1.0000 0.09 0
ZS(K) XL YL CHORD THICK TWIST NEWSEC
7.8095 -0.5 0.0 1.0000 1.0000 0.00 0
ZS(K) XL YL CHORD THICK TWIST NEWSEC
8.3043 -0.47515 0.0 0.9503 1.0000 -0.55 0
ZS(K) XL YL CHORD THICK TWIST NEWSEC
8.8778 -0.44615 0.0 0.8923 1.0000 -1.11 0
ZS(K) XL YL CHORD THICK TWIST NEWSEC
9.4513 -0.4172 0.0 0.8344 1.0000 -1.55 0
ZS(K) XL YL CHORD THICK TWIST NEWSEC
10.0228 -0.3882 0.0 0.7764 1.0000 -1.84 0
ZS(K) XL YL CHORD THICK TWIST NEWSEC
10.4141 -0.36855 0.0 0.7371 1.0000 -2.00 0

APPENDIX F

CFD Solver Input File For 7 m/s Case

```
  NREL Horizontal Axis Wind Turbine-- Phase No: and Case No.
        6  2
CONTROL FLAGS
 IRSTRT     IPRCP    IPRALL    NSTP   WW    WWIF    NSSOlVE
   0        600       1       18000     .1    10.  2
GRID SIZE/ZONE SIZE
   JST    IMTC1   IMTC2    KL(1)   KU(1)    KL(2)    KU(2)
   2       1       129      1       41       1       41
     ILE      ITE(1) ITE(2)       JROOT     JTIP
      65       26     104          8         67
FLOW CONDITION
   ADVRAT     AMTIP    REYTIP  IFIXW  Vortexes
   0.184573326979  0.111643528  1.25476488  0       2
FLOW PROPERTIES
IROE  ITURB    LTHIN  KVIS  ITRNS
3      2         0     25    0
  ITN/REV    ICONV
  36000      0
ZONAL BOUNDARY CONDITION TYPE
 IFNBCT    INFBCT
   1         2
WAKE MODEL
 IRWORFW      IWM    WUPDEG
    1         1      2.
ROTOR/BLADE MOTION
 P/F  TH1C   TH1S   BT1C   BT1S   DBTMAX   DBTMIN   DTHMAX   DTHMIN
 0    1.84  -7.5     0.     0.   0.       0.     9.       -9.
 YTIP      ALFA          ALFAL   PSI0   TWIST   SOLDTY      THCO
 10.41410   90.     0.     0.       0.   -33.     0.08706    0.005
```

APPENDIX G

NREL Phase VI Rotor Thrust Data [5]

Wind Speed (m/s)	Thrust (N)
0.4	-139.95
0.9	-114.22
1.3	-68.58
1.8	-26.6
2.2	25.3
2.7	95.32
3.1	163.3
3.6	247.7
4	338.58
4.5	435.49
4.9	537.14
5.4	642.39
5.8	751.66
6.3	864.02
6.7	978.08
7.2	1088.37
7.6	1184.66
8	1258.15
8.5	1313.71
8.9	1362.73
9.4	1407.05
9.8	1446.7
10.3	1486.94
10.7	1518.75
11.2	1547.45
11.6	1571.14
12.1	1593.53
12.5	1613.76
13	1636.27
13.4	1658.64
13.9	1681.85
14.3	1704.49
14.8	1721.54
15.2	1742.41
15.6	1772.34
16.1	1790.5
16.5	1823.83
17	1857.73
17.4	1895.33
17.9	1917.64

REFERENCES

[1] "USDA & DOE Release National Biofuels Action Plan." U.S. Department of Energy. 31 Oct. 2008 <http://www.energy.gov/news/6633.htm>.

[2] "Summary Tables Overview." DSIRE: Summary Tables. 2007. 5 Feb. 2008 http://www.dsireusa.org/summarytables/.

[3] "Wind Power Outlook 2008." American Wind Energy Association. 31 Oct. 2008 <http://www.awea.org/pubs/documents/Outlook_2008.pdf>.

[4] "What Does a Wind Turbine Cost?" Windpower. 12 May 2003. Danish Wind Industry Association. 5 Feb. 2008

[5] NREL. NREL 10-m Wind Turbine Testing in NASA Ames 80'x120' Wind Tunnel. 24 Mar. 2008 <http://wind.nrel.gov/amestest/>.

[6] PROPID. Vers. 3.4. 12 Mar. 2008 http://www.ae.uiuc.edu/m-selig/propid/.

[7] Tongchitpakdee, C., Benjanirat, C., and Sankar, L. N., "Numerical Studies of the Effects of Active and Passive Circulation Enhancement Concepts on Wind Turbine Performance," Journal of Solar Energy Engineering, Vol. 128, No. 4, November 2006.

[8] Sorensen, N. N., Michelsen, J.A., Schreck, S. (2002). "Navier-Stokes Predictions of the NREL Phase VI Rotor in the NASA Ames 80 ft x 120 ft Wind Tunnel." Wind Energy **5**: 19.

[9] Gupta, S., Leishman, J. Gordon (2006). "Performance Predictions Of The NREL Phase VI Combined Experiment Rotor Using A Free-Vortex Wake Model." AIAA **2006-390**: 21.

[10] Park, Y. M., Chang, Byeong-Hee (2007). "Numerical Simulation of Wind Turbine Scale Effects By Using CFD." AIAA **2007-216**: 10.

[11] Schmitz, S., Chattot, Jean-Jacques (2005). "Application of a 'Parallelized Coupled Navier-Stokes/Vortex-Panel Solver' to the NREL Phase VI Rotor." AIAA **2005-593**: 13.

[12] Massouh, F., Dobrev, Ivan, Rapin, Marc (2006). "Numerical Simulation of Wind Turbine Performance Using a Hybrid Model." AIAA **2006-782**: 10.

[13] Duque, E. P. N., Burklund, Michael D., Johnson, Wayne (2003). "Navier-Stokes And Comprehensive Analysis Performance Predictions Of The NREL Phase VI Experiment." AIAA **2003-0355**: 19.

[14] Benjanirat, S., Sankar, L. N., "Evaluation of a two-equation turbulence model for the Prediction of Wind Turbine Aerodynamics," Proceedings of the 22nd ASME Wind Energy Symposium, January 2003.

[15] Giguere, P., Selig, M.S. (1997). "Desirable Airfoil Characteristics for Large Variable-Speed Horizontal Axis Wind Turbines." Journal of Solar Energy Engineering **119**: 8.